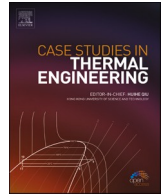




ELSEVIER

Contents lists available at ScienceDirect

Case Studies in Thermal Engineering

journal homepage: www.elsevier.com/locate/csited

Mixed convection of thermomicro-polar AgNPs-GrNPs nanofluid: An application of mass-based hybrid nanofluid model

Saeed Dinarvand^{a,*}, Mahmoud Behrouz^a, Salar Ahmadi^a, Parsa Ghasemi^a,
Samad Noeiaghdam^{b,**}, Unai Fernandez-Gamiz^c

^a Department of Mechanical Engineering, Central Tehran Branch, Islamic Azad University, Tehran, Iran

^b Industrial Mathematics Laboratory, Baikalsk School of BRICS, Irkutsk National Research Technical University, Irkutsk, 664074, Russia

^c Nuclear Engineering and Fluid Mechanics Department, University of the Basque Country UPV/EHU, Nieves Cano 12, 01006, Vitoria-Gasteiz, Spain

ARTICLE INFO

Handling Editor: Huihe Qiu

Keywords:

TMBNF
AgNPs and GrNPs
Mixed convective flow
Tiwari-Das model
Angular velocity

ABSTRACT

Here, a mass-based hybridity model is applied to inquire about the mixed convection of a thermomicro-polar binary nanofluid (TMBNF) upon a shrinking and porous plate. The nanoparticles are the silver (AgNPs) and the graphene (GrNPs), in a spherical shape, suspended in an aqua base fluid. The applied methodology considers the masses of base fluid and nanoparticles as an alternative to the first and second nanoparticles volume fraction, according to the single-phase approach named the Tiwari-Das model. By using the similarity transformation technique, the dominating PDEs are changed to a system of ODEs that can be solved numerically by the bvp4c pattern of Matlab. To validate the numerical method, a comparison is implemented for the heat transfer, the shear stress, and the gradient of microrotation values, with results reported previously that consequently a supreme agreement is observed. The variations of the angular velocity, velocity, temperature distribution, gradient of microrotation, shear stress, and the heat transfer of the TMBNF with the prominent parameters are presented and analyzed by the tabular and graphical results. The originality of this work is related to the use of the mass-based model for TMBNF flow and the derivation of a new configuration of governing equations. It is concluded that the mass-based model with its significant benefits can be utilized successfully with tremendous assurance to abundant theoretical problems of micropolar binary nanofluid flow and heat transfer. New models for the nanofluid hybridity can undoubtedly be quite helpful in the many fields where cooling technologies are essential.

1. Introduction

The power density that challenges the current cooling techniques has significantly improved due to the quick advancements in producing potentials and component minimization. Numerous research initiatives have been carried out in the past to improve the rate of heat transfer using various active or passive techniques, including porous medium [1], micro-tubes [2], fins [3], cooling systems [4], maker of vortex [5], and free convection approaches [6]. The modest thermal conductance of traditional fluid (ethylene-glycol, water, etc) constrained their ability to transmit heat, but the aforementioned approaches have given a notable improvement. A traditional fluid's thermophysical characteristics, on the other hand, may be changed to significantly improve heat transfer. Following the

* Corresponding author.

** Corresponding author.

E-mail addresses: sae.dinarvand@iauctb.ac.ir, saeed.dinarvand@yahoo.com (S. Dinarvand), snoei@istu.edu (S. Noeiaghdam).

<https://doi.org/10.1016/j.csited.2023.103224>

Received 21 February 2023; Received in revised form 16 May 2023; Accepted 22 June 2023

Available online 24 June 2023

2214-157X/© 2023 The Authors. Published by Elsevier Ltd. This is an open access article under the CC BY license (<http://creativecommons.org/licenses/by/4.0/>).

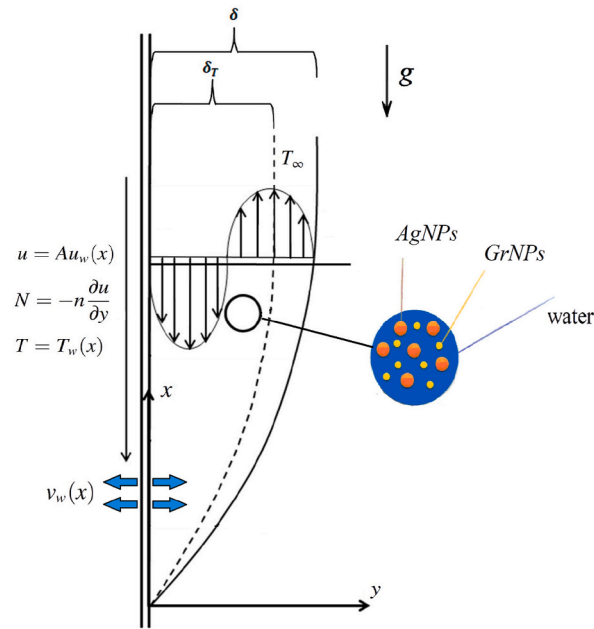


Fig. 1. Flow configuration, nanoparticles, and the conditions on the wall.

presentation of the idea of scattering of particles in the base liquid and Choi's naming of the resulting exceptionally effective heat transfer fluid as a "nanofluid" [7], many researchers have become fascinated with the exploration of nanofluids. This is due to their enhanced thermophysical characteristics and wide range of applications, including refrigeration system, solar collectors, heat exchanger, air conditioning, radiators, heat pipes, industrial thermal storage system, electronic cooling, etc. [8–10]. Using the idea of nanofluids, hybrid nanofluids are the mixing of two discordant non-metals or metal nanoparticles in the widely used heat transfer fluids. Hybrid nanofluids may be used for a variety of purposes, including improved heat exchangers, biomedical usages, microscopic, acoustics, solar systems, micro electrical, and micro-fluid, as well as naval structures, defense, propulsive, transportation, and manufacturing [11–13].

The Newtonian fluid theory states that some fluids, such as polymeric suspension, colloidal fluids, lubricants, crystals, biological fluids, slurries, paints, custard, and blood, do not obey the lineal stress-velocity gradient relation. Among all non-Newtonian fluids, the micropolar fluid has special situation in scientific debates. The idea of micropolar fluid was firstly remarked by Eringen [14], which introduced the angular momentum equation using the traditional Navier Stokes equations. Eringen expanded this idea by taking into account the heat effect and establishing the thermomicropolar fluids hypothesis [15]. Gorla [16] studied the flow on stretching/shrinking walls by 2D boundary layer equations. The thermomicropolar fluid flow across a perpendicular sheet was analyzed by Jena and Mathur through similarity relations and equations of buoyancy-driven flow [17]. As well, the effects of suction or injection with nonlinear temperature conditions, on thermomicropolar fluid flow upon a perpendicular plate investigated by them again [18]. The mixed convection upon an upright surface in a micropolar fluid was studied by Ishak et al. [19]. Micropolar nanofluid on a shrinking surface with the efficacy of magnetic field has been researched by lund et al. [20]. Hsiao [21], by taking into account the effects of magnetic field and viscous dissipation, explored micropolar nanofluid flow over a stretching sheet. The compound influences of Navier slip and magnetic field on flow over a vertical surface of an aqua nanofluid were researched by khan et al. [22]. The efficacies of radiation on the flow of micropolar fluid crossing a permeable surface were researched by Bhattacharyya et al. [23]. Al-Sanea [24] explored the convective specifications of a continually mobile wall of pulled out material near and very downstream from the extrusion slit.

Motivated by the above investigations, we attempt to explore the mixed convection of a TMBNF over a shrinking surface through mass-based model. Many scientists have been interested in the study of nanofluids in fraction-based form. The mass-based concept was initially introduced by Dinarvand [25,26]. The base of this approach is the model with a one-phase binary nanofluid which proposes base fluid mass in addition nanoparticles masses as the needed inputs to receive the efficacious physical features of binary nanofluid [27–29]. The ultimate similarity ODEs with appropriate boundary conditions are numerically solved using Matlab's bvp4c pattern for particular ratios of the controlling parameters. Additionally, after attaining a decent agreement between our computing outcomes and earlier reports, the effect of controlling factors on the flow is shown and analyzed.

2. Problem explanation with mathematical framework

Here, the 2D incompressible quiescent fluid flow of a thermomicropolar hybrid nanofluid on the shrinking sheet with suction and convection boundary condition has been considered. The x -axis is chosen along the surface whilst the y -axis is upright to it effects as displayed in Fig. 1. In addition, the linear shrinking/stretching velocity of the wall is $u_w(x) = cx$ in which $c > 0$ relates to stretching

Table 1

Models of viscosity, density, heat capacity, thermal diffusivity, thermal conductivity and thermal expansion capacity for hybrid nanofluid [25,26,30,33].

Property	Relation for hybrid Nanofluid
Viscosity (μ_{hnf})	$\frac{\mu_f}{(1 - \varphi)^{2.5}}$
Density (ρ_{hnf})	$\varphi_1\rho_1 + \varphi_2\rho_2 + (1 - \varphi)\rho_f$
Heat capacity ($(\rho C_p)_{hnf}$)	$\varphi_1(\rho C_p)_1 + \varphi_2(\rho C_p)_2 + (1 - \varphi)(\rho C_p)_f$
Thermal conductivity (k_{hnf})	$\frac{(k_{hp} + 2k_f) - 2\varphi(k_f - k_{hp})}{(k_{hp} + 2k_f) + \varphi(k_f - k_{hp})} \times (k_f), k_{hp} = \frac{\varphi_1 k_1 + \varphi_2 k_2}{\varphi_1 + \varphi_2}$
Thermal diffusivity (α_{hnf})	$\frac{k_{hnf}}{(\rho C_p)_{hnf}}$
Thermal expansion capacity ($(\rho\beta)_{hnf}$)	$\varphi_1(\rho\beta)_1 + \varphi_2(\rho\beta)_2 + (1 - \varphi)(\rho\beta)_f$

Table 2

Features of H_2O , AgNPs and GrNPs [11,34].

Thermophysical properties	Pure water	Silver (AgNPs)	Graphene (GrNPs)
ρ ($kg.m^{-3}$)	997.1	10500	2250
k ($W.m^{-1}.K^{-1}$)	0.613	429	2500
C_p ($J.kg^{-1}.K^{-1}$)	4179	235	2100
$\beta \times 10^5$ (K^{-1})	21	1.3	21
Particle size (nm)	-	2-5	10-30

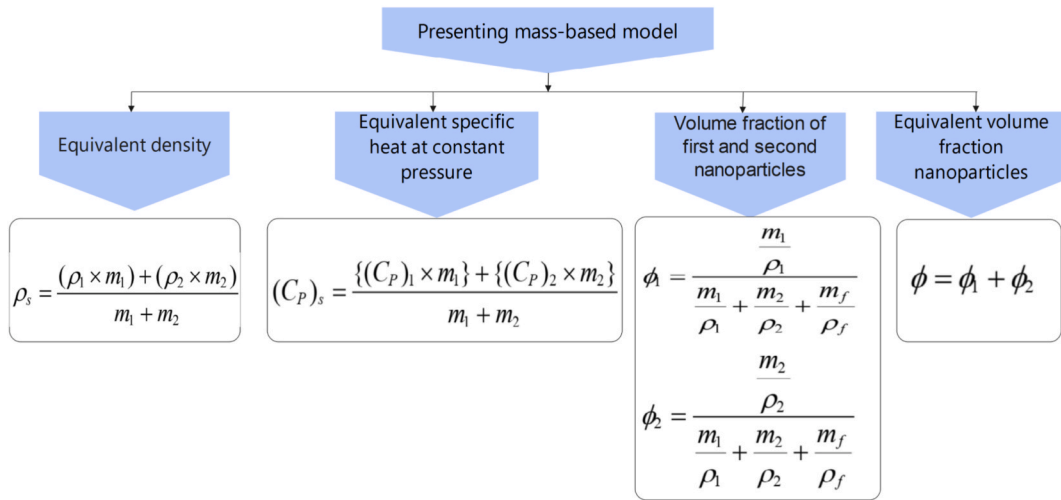


Fig. 2. Governing relations of mass-based modeling for hybrid nanofluid [25-27].

state, while $c < 0$ pretains to shrinking case. Two models are that assistance transport phenomenon, only. The first of them that is a two-phase model and explained as velocity of flow is the whole of base fluid and the slip velocity is recognized as Buongiorno model [3]. The second model is a single phase one named as Tiwari and Das model [24]. In the second model, to investigate the fluid dynamic and thermal behavior of some hybrid nanofluids, is employed here. It is supposed that solid phase (silver (AgNPs) as well as graphene (GrNPs)) and fluid phase (pure H_2O) are in thermal equivalence and no slip occurs amongst them and the features of the original fluid and the nanoparticles are supposed to be constant.

In this method of hybridity, the silver is firstly added into original fluid to appearance nanofluid, and then graphene is scattered inside nanofluid (as a new base fluid, AgNps/water) for developing the selective thermomicro-polar hybrid nanofluid [25,26]. By usual Boussinesq approximation and under above-mentioned considerations, the continuity, momentum, angular momentum and energy for the TMPBN may be inscribed as [27,30]:

$$\frac{\partial u}{\partial x} + \frac{\partial v}{\partial y} = 0, \tag{1}$$

$$u \frac{\partial u}{\partial x} + v \frac{\partial u}{\partial y} = \frac{\mu_{hnf}}{\rho_{hnf}} \frac{\partial^2 u}{\partial y^2} + \frac{\kappa}{\rho_{hnf}} \frac{\partial N}{\partial y} - g \frac{(\rho\beta)_{hnf}}{\rho_{hnf}} (T - T_\infty), \tag{2}$$

$$u \frac{\partial N}{\partial x} + v \frac{\partial N}{\partial y} = \frac{1}{\rho_{hmf}} \left(\mu_{hmf} + \frac{\kappa}{2} \right) \frac{\partial^2 N}{\partial y^2} - \frac{\kappa}{\rho_{hmf} j} \left(2N + \frac{\partial u}{\partial y} \right), \tag{3}$$

$$u \frac{\partial T}{\partial x} + v \frac{\partial T}{\partial y} = \alpha_{hmf} \frac{\partial^2 T}{\partial y^2} + \frac{D}{(\rho C)_{hmf}} \left(\frac{\partial T}{\partial x} \frac{\partial N}{\partial y} - \frac{\partial T}{\partial y} \frac{\partial N}{\partial x} \right). \tag{4}$$

Confined with this boundary conditions [27,30].

$$u = Au_w(x), v = v_w(x), N = -n \frac{\partial u}{\partial y}, T = T_\infty + T_0 x \quad \text{at } y = 0, \tag{5}$$

$$u = 0, N = 0, T = T_\infty \quad \text{when } y \rightarrow \infty.$$

In the boundary conditions, $v_w(x)$ is the mass flux via the surface, $u_w(x) = cx$ is the velocity of the shrinking wall ($c > 0$) related to the shrinking parameter ($A < 0$) [30,31]. We mention that n is a constant so that $0 \leq n \leq 1$. The state $n=0$ demonstrates $N=0$ on the surface and is thus like the no slip condition [17,18]. The item $n=1$ is applied for the turbulent flows, which is proposed by Peddieson [32]. The models that applied for thermophysical attributes of the hybrid nanofluid are as shown in Table 1. Here, the subscripts $f, 1, 2$ represent the values of the base fluid, silver nanoparticles and graphene nanoparticles, respectively. The thermophysical features of nanoparticles (AgNPs and GrNPs) and the base liquid are presented in Table 2.

For AgNPs-GrNPs/water nanofluid; we can offer our mass-based formulation model according to Fig. 2. Here, we have 5 equations and 8 unknown, (i.e. $\varphi_1, \varphi_2, \varphi, m_1, m_2, m_f, \rho_s$ and $(Cp)_s$ versus $(Cp)_1, (Cp)_2, \rho_1, \rho_2$ and ρ_f).

Now, we present the similarity transmutations for the existing problem as [27,30]:

$$\psi = (\nu_f c)^{1/2} x f(\eta), N = c \left(\frac{c}{\nu_f} \right)^{1/2} x g(\eta), \theta(\eta) = \frac{T - T_\infty}{T_w - T_\infty}, \tag{6}$$

$$\eta = \left(\frac{c}{\nu_f} \right)^{1/2} y, u = \frac{\partial \psi}{\partial x} = cx \frac{df}{d\eta}(\eta), v = \frac{\partial \psi}{\partial y} = -(c\nu_f)^{1/2} f(\eta).$$

Applying Eq. (6), the governing Eqs. (1)–(4) transform to following form:

$$f''' - \frac{1}{A_1(1 + A_2 K)} \{ (f')^2 + f f'' + A_3 K g' + Ri A_4 \theta \} = 0, \tag{7}$$

$$g'' + \frac{1}{A_1(1 + \frac{A_2 K}{2})} \{ f g' - g f' - A_3 K B(2g + f'') \} = 0, \tag{8}$$

$$A_1 = \left(1 - \frac{\frac{m_1 + m_2}{\rho_1 + \rho_2}}{\frac{m_1 + m_2 + m_f}{\rho_1 + \rho_2 + \rho_f}} \right)^{-2.5} \left\{ 1 - \frac{\frac{m_1 + m_2 + m_1 + m_2}{\rho_1 + \rho_2 + \rho_f}}{\frac{m_1 + m_2 + m_f}{\rho_1 + \rho_2 + \rho_f}} \right\}^{-1}, A_2 = \left(1 - \frac{\frac{m_1 + m_2}{\rho_1 + \rho_2}}{\frac{m_1 + m_2 + m_f}{\rho_1 + \rho_2 + \rho_f}} \right)^{2.5}$$

$$A_3 = \left\{ 1 - \frac{\frac{m_1 + m_2 + m_1 + m_2}{\rho_1 + \rho_2 + \rho_f}}{\frac{m_1 + m_2 + m_f}{\rho_1 + \rho_2 + \rho_f}} \right\}^{-1}, A_4 = A_3 \left\{ 1 - \frac{\frac{m_1 + m_2}{\rho_1 + \rho_2}}{\frac{m_1 + m_2 + m_f}{\rho_1 + \rho_2 + \rho_f}} + \frac{\rho_1 \beta_1}{\rho_f \beta_f} \left(\frac{\frac{m_1}{\rho_1}}{\frac{m_1 + m_2 + m_f}{\rho_1 + \rho_2 + \rho_f}} \right) + \frac{\rho_2 \beta_2}{\rho_f \beta_f} \left(\frac{\frac{m_2}{\rho_2}}{\frac{m_1 + m_2 + m_f}{\rho_1 + \rho_2 + \rho_f}} \right) \right\},$$

$$\theta'' + Pr \frac{\alpha_f}{\alpha_{hmf}} \{ f \theta' - \theta f' + A_5 \delta (\theta g' - g \theta') \} = 0, \tag{9}$$

$$A_5 = \left\{ \left(1 - \left(\frac{\frac{m_1 + m_2}{\rho_1 + \rho_2}}{\frac{m_1 + m_2 + m_f}{\rho_1 + \rho_2 + \rho_f}} \right) \right) + \left(\frac{\rho_1 Cp_1}{\rho_f Cp_f} \left(\frac{\frac{m_1}{\rho_1}}{\frac{m_1 + m_2 + m_f}{\rho_1 + \rho_2 + \rho_f}} \right) + \frac{\rho_2 Cp_2}{\rho_f Cp_f} \left(\frac{\frac{m_2}{\rho_2}}{\frac{m_1 + m_2 + m_f}{\rho_1 + \rho_2 + \rho_f}} \right) \right) \right\}^{-1}.$$

In like manner, the relative boundary conditions may be written as:

$$f(0) = S, f'(0) = A, g(0) = -\frac{1}{2} f''(0), \theta(0) = 1, \text{ at } \eta = 0, \tag{10}$$

$$f'(\infty) = 0, g(\infty) = 0, \theta(\infty) = 0, \text{ at } \eta \rightarrow \infty.$$

Here, the emerging parameters are the Prandtl number (Pr), the suction/injection parameter (S), the Richardson number (Ri), the micropolar heat conduction parameter (δ), the microinertia parameter (B), and the shrinking parameter (A) that their relations can be presented as

Table 3
Shear stress, gradient of microrotation, and heat transfer for thermomicrofluid and comparison with previously reported results by Roy (Fraction-based model) [30].

S	δ	A	K	Ri	B	Pr	Roy [30]			Present work						
							φ_1	φ_2	$f''(0)$	$-g(0)$	$-\dot{\theta}(0)$	m_1	m_2	$f''(0)$	$-g(0)$	$-\dot{\theta}(0)$
3.2	1	-1	0.25	1	1	6.2	0.05	0	2.523871	-3.254821	21.568212	21	0	2.523864	-3.254836	21.568222
							0.1	0	2.520325	-3.236784	17.021564	45	0	2.520322	-3.236756	17.021534
							0	0.05	3.102564	-5.056671	22.856201	0	47	3.102555	-5.056678	22.856225
							0	0.1	3.638513	-6.686541	19.651284	0	99.5	3.638526	-6.686525	19.651275

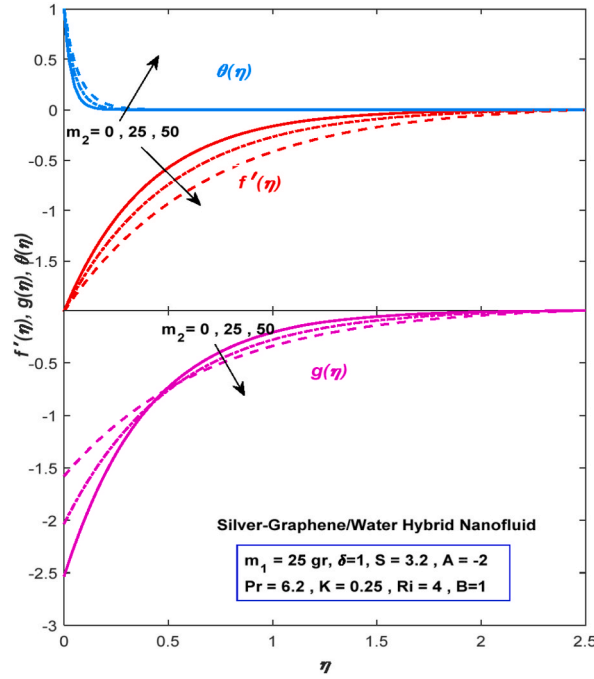


Fig. 3. The effect of m_2 on angular velocity, velocity, and temperature, when $K = 0.25, m_1 = 25\text{gr}, A = -2, Pr = 6.2, \delta = 1, B = 1, S = 3.2$.

$$S = \frac{-v_w}{(c\nu_f)^{1/2}}, M = \frac{\sigma B_0^2}{\rho_f c}, Pr = \frac{v_f(\rho C_p)_f}{k_f},$$

$$Ri = \frac{g(\rho\beta)_f(T_w - T_\infty)}{c^2}, \delta = \frac{cN^*}{v_f(\rho C)_f}, B = \frac{\nu_f}{(j_c)}, K = \frac{\kappa}{\eta_f}.$$

We emphasize that $S > 0$ illustrates the suction case, while $S < 0$ shows the injection one. Finally, C_f and Nu_x also can be given according to the following relations [17,20]:

$$C_f = \frac{(\mu_{hnf} + \kappa) \left(\frac{\partial u}{\partial y} \right)_{y=0} + (\kappa N)_{y=0}}{\rho_f \cdot U_w^2},$$

$$Nu_x = \frac{-x k_{hnf} \left(\frac{\partial T}{\partial y} \right)_{y=0}}{k_f (T_w - T_\infty)}.$$

That can be transformed to below form by applying Eq. (6).

$$[Re_x]^{1/2} C_f = \left\{ \left(1 - \frac{\frac{m_1}{\rho_1} + \frac{m_2}{\rho_2}}{\frac{m_1}{\rho_1} + \frac{m_2}{\rho_2} + \frac{m_f}{\rho_f}} \right)^{-2.5} + K \right\} f''(0) + Kg(0),$$

$$[Re_x]^{1/2} Nu_x = \frac{k_{hnf}}{k_f} \theta'(0),$$

Here, $Re_x = U_w x / \nu_f$ denotes the Reynold number.

3. Validation and numerical technique

The boundary conditions (10) and similarity governing Eqs. (7)–(9) demonstrate a substantially nonlinear character, making it difficult to determine an exact solution or closed form for this issue. As a result, the function of bvp4c from MATLAB may be used to numerically solve the existing nonlinear equations [35]. Parameters might typically emerge as the actual model is determined, or they might be added misleadingly as a feature of the solution procedure, e.g., on the off chance that there are solitary coefficients or the issue is presented on an infinite boundary. Unlike many other solvers, the bvp4c (current method) directly accepts problems with unknown parameters. To utilize the bvp4c procedure, the boundary value problems must be recast as a collection of first-order ODEs.

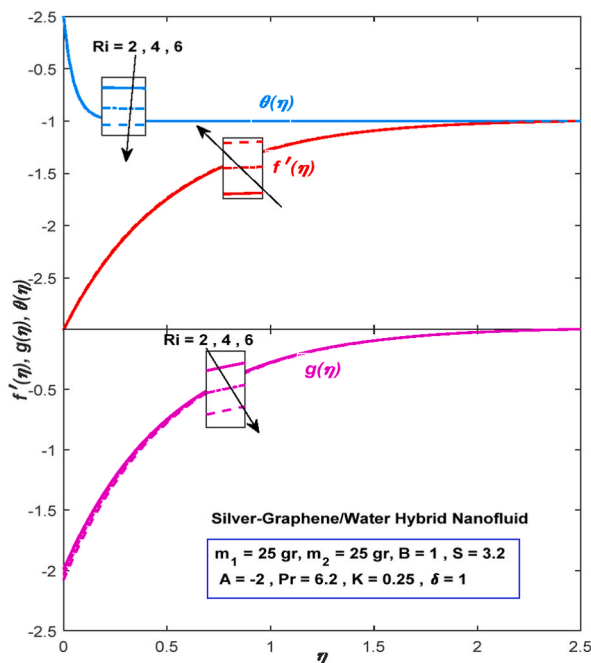


Fig. 4. The effect of Ri on angular velocity, velocity, and temperature, when $K = 0.25, m_1 = m_2 = 25\text{gr}, A = -2, Pr = 6.2, \delta = 1, B = 1, S = 3.2$.

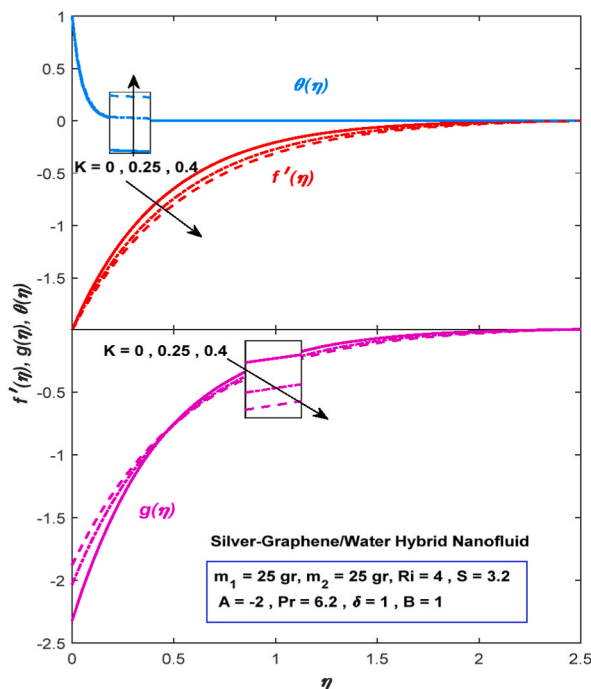


Fig. 5. The effect of K on angular velocity, velocity, and temperature, when $Ri = 4, m_1 = m_2 = 25\text{gr}, A = -2, Pr = 6.2, \delta = 1, B = 1, S = 3.2$.

The `bvp4c` needs an initial guess for the reply of the ODEs (7)-(9). The guess should demonstrate how the solution is handled and persuade the boundary conditions. The issue is first addressed for groups of parameter quantities for which the answer is straightforward. The obtained answer is then used as a first estimate to solve the issue with minimum modification to the settings. This may be done over and over again until their precise values [36–39].

Table 3 is presented to validate the applied computational method. This table shows the amount of the gradient of microrotation, the shear stress, and heat transfer for thermomicropolar nanofluent and compares with previously reported results by Roy [30].

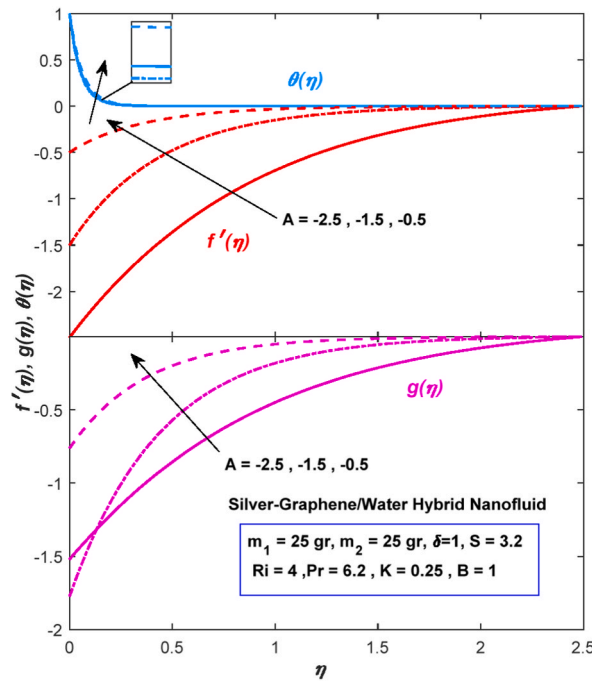


Fig. 6. The effect of A on angular velocity, velocity, and temperature, when $Ri = 4, m_1 = m_2 = 25gr, K = 0.25, Pr = 6.2, \delta = 1, B = 1, S = 3.2$.

Consequently, Table 3 implies that the existing mass-based resultants with former similar single-phase work based on volume fraction, are in fine agreement.

4. Results and discussion

4.1. Analysis of temperature and velocities components

In this section, the boundary layer behavior of velocity, microrotation and temperature will be studied and discussed. According to Tiwari and Das model [24,40–43], the results in this article, have been calculated for $0 \leq \eta \leq 0.2$. The effects of the graphene nanoparticles mass (second particle) on the angular velocity $g(\eta)$, velocity $f'(\eta)$, and temperature $\theta(\eta)$ are displayed in Fig. 3. This figure clearly shows that the temperature and velocity increase with the augment of m_2 . But in the diagram of $g(\eta)$, nearby the $\eta = 0.5$, there is an inflection point that treatment of angular velocity shows reduction before and conversely after it. Inserting the nanoparticles of Gr demonstrates a light influence on profiles of $f'(\eta), g(\eta)$, and $\theta(\eta)$. (See Khan et al. [31]). In these plots we can see that $\theta(\infty) \rightarrow 0, f'(\infty) \rightarrow 1$ and $g(\infty) \rightarrow 0$ (10) as far field boundary conditions, are well pleased alternatively which advocate the validity of the numerical results. The energy is scattered in the form of heat physically; owing to the effect of the second nanoparticle Gr, thus the temperature is increased in the boundary layer.

The effect of Ri on the temperature and velocities components are illustrated in Fig. 4. In spite of the fact that an immaterial impact is of Ri on the stream properties, a bit of diminish can be seen within the temperature and angular velocity whereas a small increase in velocity is appeared. Besides, any inflection point can not be seen on the angular velocity profile. Additionally, Lund et al. [20] explored the influence of the Richardson number on the temperature profiles and velocity and come about in a smaller-than-expected increase within the thermal boundary layer when Ri is upgraded.

For various values of the material parameter, K , the angular velocity, velocity, and temperature are showed in Fig. 5. The present figure clearly illustrates when the material parameter enhances, the velocity and temperature decrease and increase, respectively. Moreover, an inflection point is observable in the profile of angular velocity. The behavior of this profile changes before and after this point with enhancement and decrement, respectively. The reader can refer to Bhattacharyya et al. [23] for more description. Mahmood et al. [44] apperceived that as K increases, the temperature outline also enhances too. It is substantial to mention here that with the enhancement in K , thermal boundary layer thickness grows but in status of temperature gradient at the wall the effect is quite opposite.

Fig. 6 is plotted to show how velocities and temperature change with the shrinking parameter. An important point to note is that no inflection point can be seen in angular velocity. In Ref. [45], the same results about thermal and hydrodynamics boundary layers with the change in the shrinking parameter have been reported. At the surface, the function $\theta(\eta)$ have positive gradient and the profiles reduce gently to zero and decreases suddenly from an amount of one as η increases. Physically, it shows that at the inception, the heat slowly spreads from the wall to the fluid and the wall's temperature is higher than fluid.

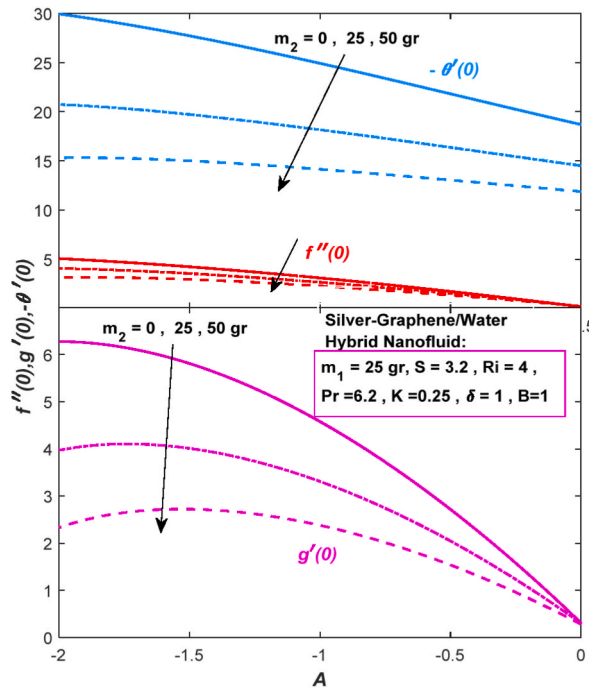


Fig. 7. Influence of m_2 on gradient of microrotation, shear stress and heat transfer, when $Ri = 4, m_1 = 25\text{gr}, S = 3.2, K = 0.25, Pr = 6.2, \delta = 1, B = 1$.

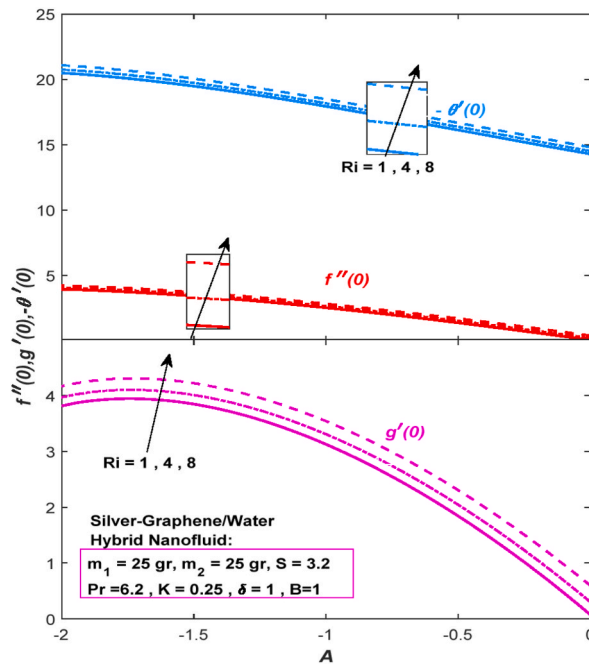


Fig. 8. Influence of Ri on gradient of microrotation, shear stress and heat transfer, when $m_1 = m_2 = 25\text{gr}, S = 3.2, K = 0.25, Pr = 6.2, \delta = 1, B = 1$.

4.2. Engineering quantities of interest

Main motivation of this section is to present and analyzed the engineering quantities of interest. Thus, Fig. 7 shows the variations of foregoing quantities as a function of shrinking parameter A for various amounts of the second nanoparticle (graphene) mass. One can see that the heat transfer, the shear stress and the gradient of microrotation enlarge in first and decrease with this parameter in continuation. Besides, for growing value of m_2 , the gradient of microrotation and shear stress enhance while heat transfer rate dramatically reduces. It is attractive mentioning that Khan et al. [31] have studied the effects of same volume fractions of distinguished

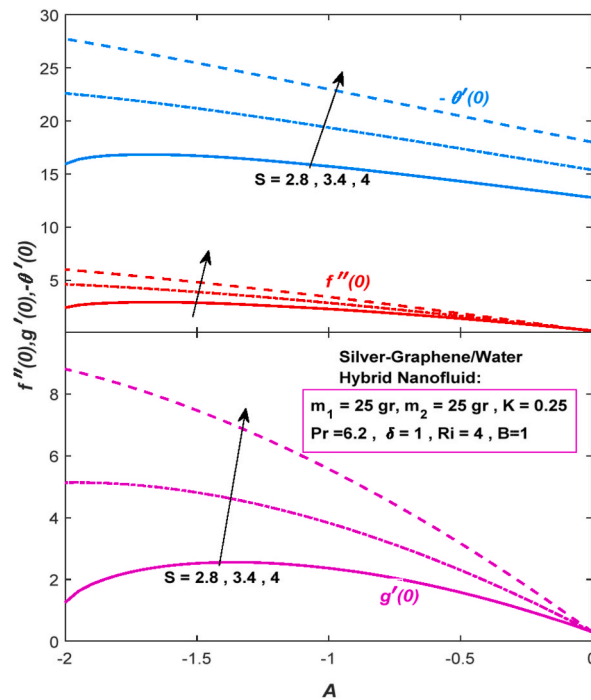


Fig. 9. Effect of S on gradient of microrotation, shear stress and heat transfer, when $m_1 = m_2 = 25$ gr, $K = 0.25$, $Ri = 4$, $Pr = 6.2$, $\delta = 1$, $B = 1$.

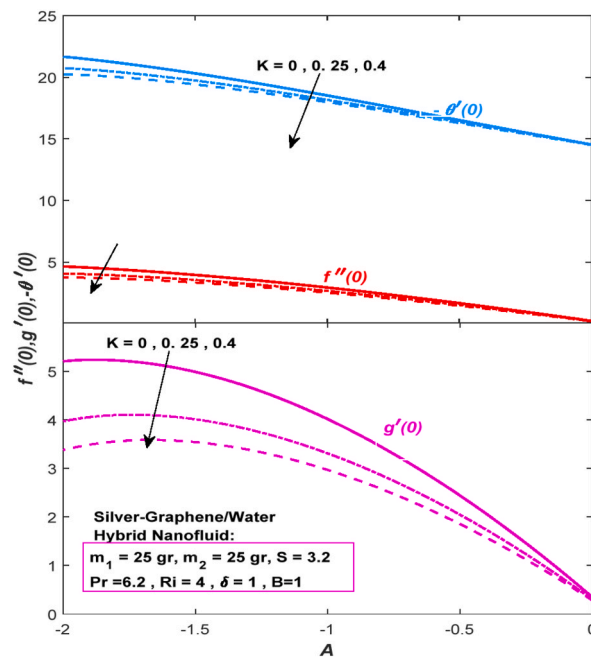


Fig. 10. Effect of K on gradient of microrotation, shear stress and heat transfer, when $m_1 = m_2 = 25$ gr, $S = 3.2$, $Ri = 4$, $Pr = 6.2$, $\delta = 1$, $B = 1$.

nanoparticles (in the present geometry) on the above-mentioned quantities, in which their results demonstrate the same behavior with present work. The heat transfer rate, the gradient of microrotation and the shear stress for diverse values of Richardson's number Ri have been plotted in Fig. 8. Here is seen a weak and increasing efficacy of Ri upon the heat transfer rate, the gradient of microrotation and the shear stress.

Fig. 9 has been plotted to present the affect of the suction parameter (S), on the heat transfer, the gradient of microrotation and the shear stress. Thinner hydrodynamic boundary layer is a result of increased suction. A surface large-velocity gradient is the result of this

problem, which increases friction. Besides, the suction speeds up the change to a turbulent flow and postpone boundary layer separation in the case of curved surfaces. For researchers to achieve their objectives, a favorable suction is typically observable. The graphical results demonstrate that a growth in the amount of S dramatically enhances the heat transfer, the gradient of microrotation and shear stress, but it can be declared that the effects of S on the shear stress is less than two other quantities. For these physical interests as a function of A , Khan et al. [31] for the $Ag-TiO_2$ /water hybrid nonoparticles in stagnation point problem with the higher value of S have observed that the conclusions first upsurges and then lessens. Moreover, like this study, they have mentioned that augmenting nanoparticles has a very little infiltration on the gradient of micro-rotation and skin friction coefficient, the rate of heat transfer. It can be predicable that augmenting S leads to the boundary layer separation becomes delay [46].

The heat transfer, the gradient of microrotation and the shear stress for the various amounts of the material parameter K are schemed in Fig. 10. To increment the value of K the foregoing quantities noticeably reduce. Anuar et al. [47] has explored numerically the unsteady flow of micropolar $Cu-Al_2O_3$ /water hybrid nanofluid accompanied by thermal radiation effect, operated by a deformable wall in stagnation region. The outcome also revealed that a rapid growth in the material parameter have been regarded to decrease the local Nusselt number of micropolar hybrid nanofluid.

5. Conclusions

In mechanical designing and fabricating activities like metal extrusions, persistent glass casting, wire drawing, and so on, the boundary layer stream caused by the stretching or shrinking wall is pivotal. In expansion, thermomicro-polar investigation can be utilized to show biological liquids like blood. Blood stream in contact with the artery divider may be an aggregate application that incorporates both stretching/shrinking wall and thermomicro-polar subjects. Also, two nanoparticles that are included in the essential liquid (blood) can be parts of a nano-based pharmaceutical. The stream of TMBNF on a vertical shrinking and penetrable wall with the mixed convection impacts in participation of latitudinal magnetic field is investigated by a numeric approach. The technique is implemented through the Tiwari-Das model, and instead of addressing the volume fraction of the first and second nanoparticles, it discusses the masses of the base fluid and nanoparticles. By utilizing a similarity transformation approach, the controlling PDEs are changed into a set of ODEs, which can be numerically solved using the Matlab bvp4c pattern. The validation is done with the formerly reported outputs that indicate a superb compromise. The effect of the emerging parameters on the angular velocity, velocity, the temperature distribution, the gradient of microrotation, the shear stress, and the heat transfer of the TMBNF is explored by the various forms of results. It was concluded that the mass-based method with its significant interests likes convenience of use and the determination of thermophysical features of TMBNF with assistance of both base fluid and nanoparticles masses may be prosperously employed to numerous theoretical problems with significant confidence. The accurate operation of the mass-based model for TMBNF flow is most considerable accomplishment of the current investigation; while the body of the paper has already provided and analyzed the details findings in depth.

Funding

The work of U.F.-G. was supported by the government of the Basque Country for the ELKARTEK21/10 KK-2021/00014 and ELKARTEK22/85 research programs, respectively.

Author statement

Saeed Dinarvand: Conceptualization, Methodology, Investigation, Supervisor. Mahmoud Behrouz: Methodology, Visualization, Writing. Salar Ahmadi: Investigation, Resources, Software. Parsa Ghasemi: Investigation, Data Curation, Writing. Samad Noeiaghdam: Methodology, Software, Visualization. Unai Fernandez-Gamiz: Conceptualization, Formal analysis, Writing-review&editing, Funding acquisition.

Declaration of competing interest

The authors declare that they have no known competing financial interests or personal relationships that could have appeared to influence the work reported in this paper.

Data availability

Data will be made available on request.

References

- [1] D. Dey, B. Chutia, Two-phase fluid motion through porous medium with volume fraction: an application of MATLAB bvp4c solver technique, *Heat transfer* 51 (2) (2022) 1778–1789.
- [2] J.R. Pattnaik, S.R. Mishra, B. Ali, P.K. Pattnaik, Investigation of asymmetric wall temperature and concentration on free convection of conducting fluid in a microchannel, *Heat transfer* 51 (1) (2022) 622–640.
- [3] I. Ahmad, H. Zahid, F. Ahmad, M.A.Z. Raja, D. Baleanu, Design of computational intelligent procedure for thermal analysis of porous fin model, *Chin. J. Phys.* 59 (2019) 641–655.
- [4] A. Peddu, S. Chakraborty, P.K. Das, Visualization and flow regime identification of downward air–water flow through a 12 mm diameter vertical tube using image analysis, *Int. J. Multiphas. Flow* 100 (2018) 1–15.

- [5] U. Kashyap, K. Das, B.K. Debnath, U. Kashyap, S.K. Saha, Numerical study on effect of secondary surface on rectangular vortex generator, *J. Therm. Sci. Eng. Appl.* 13 (1) (2021).
- [6] S. Ahmad, S. Nadeem, Thermal analysis in buoyancy driven flow of hybrid nanofluid subject to thermal radiation, *Int. J. Ambient Energy* 43 (1) (2022) 3868–3876.
- [7] S.U.S. Choi, Enhancing thermal conductivity of fluids with nanoparticles, in: *The Proceedings of the ASME International Mechanical Engineering Congress and Exposition*, vol. 66, 1995, pp. 99–105.
- [8] S. Nadeem, S. Ahmad, Al Issakhov, I.M. Alarifi, MHD stagnation point flow of nanofluid with SWCNT and MWCNT over a stretching surface driven by Arrhenius kinetics, *Applied Mathematics-A Journal of Chinese Universities* 37 (2022) 366–382.
- [9] F. Hoseinnejad, S. Dinarvand, M.E. Yazdi, Manninen's mixture model for conjugate conduction and mixed convection heat transfer of a nanofluid in a rotational/stationary circular enclosure, *Int. J. Numer. Methods Heat Fluid Flow*, 31 (5) 1662-1694.
- [10] W.F. Xia, S. Ahmad, M. Naveed Khan, H. Ahmad, A. Rehman, J. Baili, T. Nguyen Gia, Heat and mass transfer analysis of nonlinear mixed convective hybrid nanofluid flow with multiple slip boundary conditions, *Case Stud. Therm. Eng.* 32 (2022), 101893.
- [11] H. Shojaie Chahregh, S. Dinarvand, TiO₂-Ag/blood hybrid nanofluid flow through an artery with applications of drug delivery and blood circulation in the respiratory system, *Int. J. Numer. Methods Heat Fluid Flow* 30 (2020) 4775–4796.
- [12] A. Ghennai, R. Bessaïh, Heat transfer enhancement in a cubical cavity filled with a hybrid nanofluid, *Heat Transfer* 50 (2021) 1658–1678.
- [13] H. Berrehal, S. Dinarvand, I. Khan, Mass-based hybrid nanofluid model for entropy generation analysis of flow upon a convectively-warmed moving wedge, *Chin. J. Phys.* 77 (2022) 2603–2616.
- [14] A.C. Eringen, Theory of micropolar fluids, *J. Math. Mech.* 16 (1966) 1–18.
- [15] A.C. Eringen, Theory of thermomicrofluids, *J. Math. Anal. Appl.* 38 (1972) 480–496.
- [16] R.S.R. Gorla, Micropolar boundary layer at a stagnation point, *Int. J. Eng. Sci.* 21 (1) (1983) 25–34.
- [17] S.K. Jena, M.N. Mathur, Similarity solutions for laminar free convection flow of a thermomicrofluid past a non-isothermal vertical flat plate, *Int. J. Eng. Sci.* 19 (1981) 1431–1439.
- [18] S.K. Jena, M.N. Mathur, Free convection in the laminar boundary layer flow of a thermomicrofluid past a vertical plate with suction/injection, *Acta Mech.* 42 (1982) 227–238.
- [19] A. Ishak, Roslinda Nazar, Ioan Pop, Dual solutions in mixed convection boundary layer flow of micropolar fluids, *Commun. Nonlinear Sci. Numer. Simulat.* 14 (2009) 1324–1333.
- [20] L.A. Lund, Z. Omar, I. Khan, Mathematical analysis of magnetohydrodynamic (MHD) flow of micropolar nanofluid under buoyancy effects past a vertical shrinking surface: dual solutions, *Heliyon* 5 (2019), 02432.
- [21] K.L. Hsiao, Micropolar nanofluid flow with MHD and viscous dissipation effects towards a stretching sheet with multimedia feature, *Int. J. Heat Mass Tran.* 112 (2017) 983–990.
- [22] W.A. Khan, O.D. Makinde, Z.H. Khan, MHD boundary layer flow of a nanofluid containing gyrotactic microorganisms past a vertical plate with Navier slip, *Int. J. Heat Mass Tran.* 74 (2014) 285–291.
- [23] K. Bhattacharyya, S. Mukhopadhyay, G.C. Layek, I. Pop, Effects of thermal radiation on micropolar fluid flow and heat transfer over a porous shrinking sheet, *Int. J. Heat Mass Tran.* 55 (2012) 2945–2952.
- [24] S.A. Al-Sanea, Mixed convection heat transfer along a continuously moving heated vertical plate with suction or injection, *Int. J. Heat Mass Tran.* 47 (2004) 1445–1465.
- [25] S. Dinarvand, M. Nademi Rostami, An innovative mass-based model of aqueous zinc oxide–gold hybrid nanofluid for von Kármán's swirling flow, *J. Therm. Anal. Calorim.* 138 (2019) 845–855.
- [26] S. Dinarvand, M. Nademi Rostami, I. Pop, A novel hybridity model for TiO₂-CuO/water hybrid nanofluid flow over a static/moving wedge or corner, *Sci. Rep.* 9 (2019), 16290.
- [27] S.M. Mousavi, M.N. Rostami, M. Yousefi, S. Dinarvand, I. Pop, M.A. Sheremet, Dual solutions for Casson hybrid nanofluid flow due to a stretching/shrinking sheet: a new combination of theoretical and experimental models, *Chin. J. Phys.* 71 (2021) 574–588.
- [28] S. Dinarvand, S.M. Mousavi, M. Yousefi, M. Nademi Rostami, MHD flow of MgO-Ag/water hybrid nanofluid past a moving slim needle considering dual solutions: an applicable model for hot-wire anemometer analysis, *Int. J. Numer. Methods Heat Fluid Flow* 32 (2) (2022) 488–510.
- [29] S. Dinarvand, A. Mahdavi Nejad, Off-centered stagnation point flow of an experimental-based hybrid nanofluid impinging to a spinning disk with low to high non-alignments, *Int. J. Numer. Methods Heat Fluid Flow* 32 (8) (2022) 2799–2818.
- [30] N. Ch Roy, Mathematical approach of demarcation of dual solutions for a flow over a shrinking surface, *Chin. J. Phys.* 68 (2020) 514–532.
- [31] U. Khan, A. Zaib, S.A. Bakar, A. Ishak, Stagnation-point flow of a hybrid nanofluid over a non-isothermal stretching/shrinking sheet with characteristics of inertial and microstructure, *Case Stud. Therm. Eng.* 26 (2021), 101150.
- [32] J. Peddieson, An application of the micropolar fluid model to the calculation of turbulent shear flow, *Int. J. Eng. Sci.* 10 (1) (1972) 23–32.
- [33] L. Qin, S. Ahmad, M. Naveed Khan, M. Ameer Ahammad, A.M. Galal, Thermal and Solutal Transport Analysis of Blasius-Rayleigh-Stokes Flow of Hybrid Nanofluid with Convective Boundary Conditions, *Waves in Random and Complex Media*, 2022, <https://doi.org/10.1080/17455030.2022.2072018>. In Press.
- [34] B. Zhao, Z. Wang, F. Chen, Y. Yang, Y. Gao, L. Chen, Z. Jiao, L. Cheng, Y. Jiang, Three-dimensional interconnected spherical Graphene framework/SnS nanocomposite for anode material with superior lithium storage performance: complete reversibility of Li₂S, *ACS Appl. Mater. Interfaces* 9 (2) (2017) 1407–1415.
- [35] L.F. Shampine, I. Gladwell, S. Thompson, *Solving ODEs with MATLAB*, Cambridge University Press, 2003.
- [36] J.V. Tawade, C.N. Guled, S. Noeiaghdam, U. Fernandez-Gamiz, V. Govindan, S. Balamuralitharan, Effects of thermophoresis and Brownian motion for thermal and chemically reacting Casson nanofluid flow over a linearly stretching sheet, *Results Eng.* 15 (2022), 100448.
- [37] S. Arulmozhi, K. Sukkiramathi, S.S. Santra, R. Edwan, U. Fernandez-Gamiz, S. Noeiaghdam, Heat and Mass transfer analysis of Radiative and Chemical reactive effects on MHD Nanofluid over an infinite moving vertical plate, *Results Eng.* 14 (2022), 100394.
- [38] G. Dharmiah, S. Dinarvand, P. Durgaprasad, S. Noeiaghdam, Arrhenius activation energy of tangent hyperbolic nanofluid over a cone with radiation absorption, *Results Eng.* 16 (2022), 100745.
- [39] N. Hameed, S. Noeiaghdam, W. Khan, B. Pimpunchat, U. Fernandez-Gamiz, M. Sohail Khan, A. Rehman, Analytical Analysis of the Magnetic Field, Heat Generation and Absorption, Viscous Dissipation on Couple Stress Casson Hybrid Nano Fluid over a Nonlinear Stretching Surface, *Results in Engineering*, 2022.
- [40] A. Saeed, R. Ali Shah, M. Sohail Khan, U. Fernandez Gamiz, M.Z. Bani Fwaz, S. Noeiaghdam, A.M. Galal, Theoretical analysis of unsteady squeezing nanofluid flow with physical properties, *Math. Biosci. Eng.* 19 (10) (2022) 10176–10191.
- [41] A. Ghasemian, S. Dinarvand, A. Adamian, M.A. Sheremet, Unsteady general three-dimensional stagnation point flow of a maxwell/Buongiorno non-Newtonian nanofluid, *Journal of Nanofluids* 8 (7), 1544-1559.
- [42] M.S. Khan, S. Mei, Shabnam, U. Fernandez-Gamiz, S. Noeiaghdam, A. Khan, Numerical simulation of a time-dependent electroviscous and hybrid nanofluid with Darcy-forchheimer effect between squeezing plates, *Nanomaterials* 12 (2022) 876.
- [43] M.S. Khan, S. Mei, Shabnam, U. ernandez-Gamiz, S. Noeiaghdam, S.A. Shah, A. Khan, Numerical analysis of unsteady hybrid nanofluid flow comprising CNTs-ferrous oxide/water with variable magnetic field, *Nanomaterials* 12 (2022) 180.
- [44] A. Mahmood, B. Ch, A. Ghaffari, Hydromagnetic Hiemenz flow of micropolar fluid over a nonlinearly stretching/shrinking sheet: dual solutions by using Chebyshev Spectral Newton Iterative Scheme, *J. Magn. Magn Mater.* 416 (2016) 329–334.

- [45] S. Kh Soid, A. Ishak, I. Pop, Unsteady MHD flow and heat transfer over a shrinking sheet with ohmic heating, *Chin. J. Phys.* 55 (2017) 1626–1636.
- [46] M. Naveed Khan, N. Akkurt, N. Ameer Ahammad, S. Ahmad, A. Amari, S.M. Eldin, A. Ali Pasha, Irreversibility analysis of Ellis hybrid nanofluid with surface catalyzed reaction and multiple slip effects on a horizontal porous stretching cylinder, *Arab. J. Chem.* 15 (12) (2022), 104326.
- [47] N.S. Anuar, N. Bachok, Double solutions and stability analysis of micropolar hybrid nanofluid with thermal radiation impact on unsteady stagnation point flow, *Mathematics* 9 (2021) 276–289.

Nomenclature

A: shrinking parameter
 B: microinertia parameter
 c: constant
 C: heat capacity
 C_f : skin friction coefficient
 C_p : specific heat at constant pressure
 D: coefficient of micropolar heat conduction
 g: acceleration due to gravity
 h: coefficient of convective heat transfer
 hp: hybrid particle
 j: micro-inertia density
 k: thermal conductivity
 K: material parameter
 m: mass
 n: component of microrotation
 N: microrotation in the xy plane
 Nu_x : local Nusselt number
 Pr: Prandtl number
 R: radiation parameter
 Ri: Richardson number
 Re_x : local Reynolds number
 S: suction or injection parameter
 T: temperature field
 u, v: velocity components along x and y axes
 x, y: 2D Cartesian coordinates system
 n: component of microrotation

Greek symbols

ϕ : volume fraction
 β : coefficient of thermal expansion
 η : independent similarity variable
 $f(\eta)$: non-dimensional stream function
 $\theta(\eta)$: dimensionless temperature distribution
 μ : dynamic viscosity
 ν : kinematic viscosity
 ρ : density
 A_1 to A_5 : coefficients of ODE equations
 ρC_p : volumetric heat capacity at constant pressure
 κ : vortex viscosity
 δ : micropolar heat conduction parameter

Subscripts

s: equivalent property of nanoparticles
 f: base fluid
 nf: mono-nanofluid
 hnf: hybrid nanofluid
 1: first nanoparticle (Graphene)
 2: second nanoparticle (Silver)
 ∞ : Conditions in the free stream
 w: surface of the plate